JPET Fast Forward. Published on August 10, 2004 as DOI: 10.1124/jpet.104.071803

MECHANISM-BASED INACTIVATION OF HUMAN CYTOCHROME P4502C8 BY DRUGS IN VITRO

THOMAS M. POLASEK, DAVID J. ELLIOT, BENJAMIN C. LEWIS AND JOHN O. MINERS

DEPARTMENT OF CLINICAL PHARMACOLOGY, FLINDERS UNIVERSITY AND FLINDERS MEDICAL CENTRE, ADELAIDE, AUSTRALIA (T.M.P., D.J.E., B.C.L. and J.O.M.)

JPET Fast Forward. Published on August 10, 2004 as DOI: 10.1124/jpet.104.071803
This article has not been copyedited and formatted. The final version may differ from this version.

a) Running Title: Mechanism-Based Inactivation of CYP2C8

b) Corresponding Author: Professor John O. Miners, Department of Clinical Pharmacology, Flinders University and Flinders Medical Centre, Bedford Park, SA 5042, Australia. Telephone: 61-8-82044999. Fax: 61-8-82045114. Email: John.Miners@flinders.edu.au

c) Text Pages: 43

Tables: 4

Figures: 5

References: 40

Words in Abstract: 246

Words in Introduction: 676

Words in Discussion: 1508

d) Abbreviations: CYP, cytochrome(s) P450; CYP2C8, cytochrome P4502C8; MBI, mechanism-based inactivation; MBIs, mechanism-based inactivators; MIC, metabolite-intermediate complexation; HLMs, human liver microsomes; HPLC, high-performance liquid chromatography; CCBs, calcium channel blockers; TCAs, tricyclic antidepressants; MAOIs, monoamine oxidase inhibitors.

e) Recommended Section: Absorption, Distribution, Metabolism & Excretion

JPET Fast Forward. Published on August 10, 2004 as DOI: 10.1124/jpet.104.071803
This article has not been copyedited and formatted. The final version may differ from this version.

ABSTRACT

Studies were conducted to evaluate the potential mechanism-based inactivation of recombinant and human liver microsomal CYP2C8 by clinically used drugs. Several tricyclic antidepressants, calcium channel blockers, monoamine oxidase inhibitors and various other known CYP3A4 inhibitors exhibited greater inhibition of CYP2C8 (paclitaxel 6α-hydroxylation) following pre-incubation, consistent with mechanism-based inactivation. Inactivation of recombinant CYP2C8 by phenelzine, amiodarone, verapamil, nortriptyline, fluoxetine, and isoniazid was of the pseudo-first order type and was characterized by respective inactivation kinetic constants (K_I and k_{inact}) of 1.2 μM and 0.243 min^{-1}, 1.5 μM and 0.079 min^{-1}, 17.5 μM and 0.065 min^{-1}, 49.9 μM and 0.036 min^{-1}, 294 μM and 0.083 min^{-1} and 374 μM and 0.042 min^{-1}. Spectral scanning of recombinant CYP2C8 demonstrated the formation of metabolite-intermediate complexes with verapamil, nortriptyline, fluoxetine and isoniazid, but not amiodarone. In contrast, inactivation by phenelzine resulted from heme destruction by free radicals. Studies with human liver microsomes (HLMs) revealed that nortriptyline, verapamil and fluoxetine were not mechanism-based inactivators (MBIs) of CYP2C8. Simultaneous inactivation of CYP2C8 and CYP3A4 (paclitaxel 3'-phenyl-hydroxylation) was observed using amiodarone, isoniazid and phenelzine, with the efficiency of inactivation greater for the CYP3A4 pathway. With the exception of phenelzine, glutathione and superoxide dismutase failed to protect CYP2C8 (recombinant and HLMs) or CYP3A4 from inactivation by MBIs. However, the alternate CYP2C8 substrate torsemide prevented CYP2C8 inactivation in all cases. These data are consistent with mechanism-based inactivation of CYP2C8 by a range of commonly prescribed drugs, several of which have been implicated in clinically important drug-drug interactions.

JPET Fast Forward. Published on August 10, 2004 as DOI: 10.1124/jpet.104.071803
This article has not been copyedited and formatted. The final version may differ from this version.

Metabolic drug-drug interactions that arise via mechanism-based inactivation (MBI) of cytochrome P450 enzymes (CYP) have generated great interest in recent years since the reduction in metabolic clearance can be severe and long lasting (Lin and Lu, 1998). The majority of studies performed to date have focused on CYP3A4, the principal isoform involved in the metabolic clearance of drugs in humans. Drug-drug interactions involving macrolide antibiotics (Ito et al., 2003), calcium channel blockers (Ma et al., 2000), HIV protease inhibitors (Koudriakova et al., 1998), and some antidepressants (Mayhew et al., 2000) can be quantitatively better explained when the inactivation component of CYP3A4 inhibition is considered. However, it is now apparent that the function of other CYP isoforms may also be significantly impaired by drugs that act as mechanism-based inactivators (MBIs). Clinically relevant inactivation of CYP1A2 by zileuton (Lu et al., 2003), CYP2B6 by clopidogrel and ticlopidine (Richter et al., 2004), CYP2C9 by suprofen (O'Donnell et al., 2003), CYP2C19 by ticlopidine (Ha-Duong et al., 2001) and CYP2D6 by paroxetine and metoclopramide (Desta et al., 2002; Bertelsen et al., 2003) has recently been demonstrated in vitro.

In contrast to reversible inhibition, MBI requires at least one CYP catalytic cycle to produce reactive intermediate species that covalently modify the enzyme and cause impairment of function (Lin and Lu, 1998). In vitro, MBIs characteristically exhibit, 1) time dependent inactivation, 2) saturation kinetics, 3) reduced rates of inactivation in the presence of alternate substrates, 4) a 1:1 stoichiometry for inhibitor and enzyme, 5) involvement of a catalytic step, 6) inactivation of enzyme prior to release of reactive species, and 7) quasi-irreversible or irreversible loss of function (Silverman, 1988). The maximal rate constant of inactivation (k_{inact}) and the inactivator concentration required for half-maximal inactivation (K_I) are experimentally derived in

vitro kinetic constants that are useful descriptors of the potency of a drug as a MBI. The ratio of k_{inact} / K_I may additionally serve as an indicator of inactivator efficiency. In the case of CYP mediated drug-drug interactions, physiological based and non-physiological based models have incorporated these kinetic constants to predict the degree of CYP inactivation in vivo, and may provide sound estimates of the decrease in clearance when other drugs are coadministered (Mayhew et al., 2000; Ito et al., 2003).

Although the role of CYP2C8 was previously considered to be limited to the oxidation of endogenous retinoids and fatty acids, such as all-*trans*-retinoic acid and arachidonic acid, there is growing awareness of the importance of this enzyme in human drug metabolism. Interestingly, there appears to be a degree of overlapping substrate and inhibitor selectivity between CYP3A4 and CYP2C8. Thus, CYP2C8 contributes in part to the metabolism of the predominantly CYP3A4 substrates carbamazepine, verapamil and zopiclone (Ong et al., 2000). Conversely, CYP3A4 contributes to the metabolism of the predominantly CYP2C8 substrates cerivastatin and paclitaxel (Ong et al., 2000). Both isoforms also metabolize repaglinide, methadone and chloroquine (Bidstrup et al., 2003; Projean et al., 2003; Wang and DeVane, 2003). Ong et al. (2000) additionally reported that amiodarone, amitriptyline, terfenadine, quinine, midazolam and triazolam caused > 50% inhibition of CYP2C8 at concentrations corresponding to their relevant CYP3A4 K_m values, suggesting similar affinities for both enzymes. Furthermore, other CYP3A4 substrates such as nifedipine, felodipine and testosterone also appear to inhibit CYP2C8 (Harris et al., 1994).

To date, there have been no investigations of potential mechanism-based inactivation of CYP2C8. Given the overlapping substrate and inhibitor selectivities of CYP3A4 and CYP2C8, and the emerging role of CYP2C8 in the metabolism of drugs, this work aimed to: evaluate a range of CYP3A4 inhibitors and other drugs as mechanism-based inactivators of CYP2C8; characterize the kinetics of CYP2C8 inactivation; and determine the mechanisms of CYP2C8 inactivation. Drugs investigated as potential MBIs of CYP2C8 included a series of macrolide antibiotics and calcium channel blockers (CCBs), 17α-ethynylestradiol, amiodarone, fluoxetine and tamoxifen (all known MBIs of CYP3A4), and several monoamine oxidase inhibitors (MAOIs) and tricyclic antidepressants (TCAs), classes that have been implicated as MBIs in previous studies (Muakkassah et al., 1981; Bensoussan et al., 1995; Wen et al., 2002).

JPET Fast Forward. Published on August 10, 2004 as DOI: 10.1124/jpet.104.071803
This article has not been copyedited and formatted. The final version may differ from this version.

MATERIALS AND METHODS

Chemicals. Testosterone, 6β-hydroxytestosterone, paclitaxel, troleandomycin, erythromycin, roxithromycin, amitriptyline, nortriptyline, desipramine, norclomipramine, diltiazem, verapamil, nicardipine, felodipine, mibefradil, selegiline, tranylcypromine, isoniazid, phenelzine, fluoxetine, 17α-ethynylestradiol, diethylstilbestrol, 4-methylumbelliferone, trimethoprim, glucose 6-phosphate, glucose 6-phosphate dehydrogenase, β-nicotinamide adenine dinucleotide phosphate (NADP), mannitol, reduced glutathione, and superoxide dismutase were purchased from Sigma-Aldrich (Sydney, Australia). 6α-Hydroxypaclitaxel was purchased from BD Gentest (Woburn, MA, USA). Other chemicals were kindly donated by the following sources: azithromycin, Pfizer Australia (Sydney, Australia); clarithromycin, Abbott Laboratories (Chicago, IL, USA); torsemide, Boehringer Mannheim International (Mannheim, Germany); desmethylnortriptyline, F. Hoffmann-La Roche Ltd (Basel, Switzerland); amiodarone and desethylamiodarone, Sanofi UK Ltd (Manchester, England); indinavir, Merck Sharp & Dohme Pty Ltd (Sydney, Australia); tamoxifen, Imperial Chemical Industries PLC (Manchester, England); and ketoconazole, Janssen-Cilag Pty (Sydney, Australia). Restriction enzymes were purchased from New England Biolabs Inc. (Hitchin, Hertfordshire, UK) and *E. coli* DH5α cells from Life Technologies (Melbourne, Australia). All other chemicals and reagents were of analytical reagent grade.

Construction of CYP2C8, CYP3A4 and rOXR Expression Plasmids

N-Terminus modifications known to promote high levels of bacterial expression of human CYP were incorporated into the wild type CYP2C8 (accession Y00498) and CYP3A4 (accession AF182273) cDNAs (Boye et al., 2004). The N-terminal

JPET Fast Forward. Published on August 10, 2004 as DOI: 10.1124/jpet.104.071803
This article has not been copyedited and formatted. The final version may differ from this version.

membrane anchor of CYP2C8 was replaced with modified sequence derived from P45017A as previously described (Richardson et al., 1995). In addition, the bovine 17α-hydroxylase leader sequence (MALLLAVFL) was immediately followed by the cytochrome 2C consensus sequence (GLSCLLLLS). Generation of the 17α-hydroxylase leader sequence in CYP3A4 cDNA utilized PCR-directed mutagenesis to delete codons 3-10 using the following primers: Sense- 5′ TA**CATATG**GCTCTGTTATTAGCAGTTTTTCTGGTGCTCCTCTATCTATATGG 3′; antisense- 5′ AAT**GTCGAC**TCAGGCTCCACTTACGGTGCC 3′. To facilitate directional ligation into the pCW plasmid, NdeI and SalI restriction sites (bold text) were incorporated into the sense and antisense CYP3A4-oligonucleotides, respectively. The 1486 bp 17α-CYP2C8 and 1496 bp 17α-CYP3A4 PCR products were digested with NdeI/HindIII and NdeI/SalI prior to ligation into the pCW ori(+) plasmid.

The cDNA coding for rat cytochrome P450 oxidoreductase (rOxR) consisted of the OmpA signal sequence (MKKTAIAIAVALAGFATVAQA) fused upstream of the full length native rat OxR sequence. The rOxR expression construct was generated using the bacterial plasmid pACYC184, as documented previously (Boye et al., 2004).

Heterologous Co-expression of pCW-17αCYP2C8 and pCW-17αCYP3A4 with pACYC OmpA-rOXR. pCW-17αCYP2C8 and pCW-17αCYP3A4 constructs were co-transformed into DH5α *E. coli* cells with pACYC OmpA-rOXR. Ampicillin/chloramphenicol selected colonies were screened for the correct plasmid by restriction enzyme analysis. Plasmid DNA was purified with the QIAprep Spin Miniprep Kit (Qiagen) and confirmed on both strands by sequencing (ABI Prism

3100). Cells were cultured and membrane fractions separated as described (Boye et al., 2004). The total protein concentration of membrane fractions was determined (Lowry et al., 1951) and holo-enzyme quantified (Omura and Sato, 1964). The rate of reduction of cytochrome c was used as a measure of rOxR activity in membrane fractions (Yasukochi and Masters, 1976).

Human Liver Microsomes. The Flinders Medical Centre Ethics Review Committee approved the use of human liver tissue for in vitro drug metabolism studies obtained from the liver 'bank' of the Department of Clinical Pharmacology. Microsomes from six livers (H6, H7, H10, H12, H13 and H40) were prepared by differential centrifugation. Liver portions in phosphate buffer (0.1 M, pH 7.4) containing 1.15% w/v potassium chloride were homogenized sequentially with a Janke and Kunkle Ultra Tarex (24,000 rpm) and a Potter-Elvehjem homogenizer (mechanical drive at 1480 rpm). The homogenate was centrifuged at 700 g for 10 min and then at 10,000 g for a further 10 min. The supernatant fraction was aspirated and centrifuged at 105,000 g for 60 min at 4ºC. The resulting pellet was re-suspended in phosphate buffer (0.1 M, pH 7.4) containing 1.15% w/v potassium chloride and centrifuged at 105,000 g for 60 min at 4ºC. The microsomal pellet was suspended in phosphate buffer (0.1 M, pH 7.4) containing 20% glycerol and stored at –80ºC until use. Microsomal protein concentrations were determined by the method of Lowry et al. (1951) using bovine serum albumin as standard. The kinetics of testosterone and paclitaxel metabolism were determined using the microsomes from the six livers. Inhibition studies were conducted using pooled HLMs, with equal amounts of microsomal protein from each liver.

JPET Fast Forward. Published on August 10, 2004 as DOI: 10.1124/jpet.104.071803
This article has not been copyedited and formatted. The final version may differ from this version.

Inhibition of CYP3A4 and CYP2C8 in the MBI Screen. *Co-incubation*. Inhibitors were incubated with HLMs or recombinant enzyme and NADPH-regenerating system in the presence of probe substrates for 15 min (testosterone assay) or 10 min (paclitaxel assay) at 37°C. Co-incubation mixtures contained either HLMs (0.1 mg/ml), recombinant CYP3A4 (10 pmol/ml) or CYP2C8 (10 pmol/ml), NADPH-regenerating system (1 mM NADP, 10 mM glucose 6-phosphate, 2 IU/ml glucose 6-phosphate dehydrogenase, 5 mM $MgCl_2$), inhibitor, probe substrate, and phosphate buffer (0.1 M, pH 7.4) in a total volume of 500 μl (testosterone assay) or 200 μl (paclitaxel assay). Probe substrates were included at concentrations close to reaction K_m values; 40 μM testosterone using HLMs and recombinant CYP3A4 or 10 μM paclitaxel using HLMs and 1.5 μM paclitaxel using recombinant CYP2C8 (see Results). Total solvent concentration (acetonitrile for the testosterone assay and methanol for the paclitaxel assay) was either 1 or 2%. The testosterone assay was terminated by the addition of 5 μl of 70% perchloric acid and 4-methylumbelliferone (0.05 μg) was added as the internal standard. The paclitaxel assay was terminated by the addition of 200 μl of ice-cold acetonitrile containing diethylstilbestrol (0.1 μg) as the internal standard. Mixtures were vortex mixed, chilled on ice and then centrifuged (4000 g) before analysis of the supernatant fraction by HPLC. Rates of formation of all metabolites (6β-hydroxytestosterone, 6α-hydroxypaclitaxel and 3'-phenyl-hydroxypaclitaxel) were linear with respect to protein concentration and incubation time.

Pre-Incubation. Inhibitors were pre-incubated with HLMs or recombinant enzyme and NADPH-regenerating system in the absence of the probe substrates for 30 min at 37°C. A pre-incubation time of 20 min was employed for CYP3A4 studies with the

JPET Fast Forward. Published on August 10, 2004 as DOI: 10.1124/jpet.104.071803
This article has not been copyedited and formatted. The final version may differ from this version.

macrolides due to their marked effect on activity. Pre-incubation mixtures contained either HLMs (0.1 mg/ml), recombinant CYP3A4 (10 pmol/ml) or CYP2C8 (10 pmol/ml), NADPH-regenerating system, inhibitor, and phosphate buffer (0.1 M, pH 7.4) in a total volume of 500 μl (testosterone assay) or 200 μl (paclitaxel assay). Following pre-incubation, probe substrates were added at the concentrations specified for the co-incubations and the reactions allowed to proceed. Total solvent concentration (acetonitrile for the testosterone assay and methanol for the paclitaxel assay) was either 1 or 2%. Reactions were terminated and the samples were prepared for HPLC analysis as described above.

Kinetics of Paclitaxel Metabolism Inactivation. A two step incubation method was utilized to characterize the time- and concentration-dependent inhibition of paclitaxel metabolism by selected inactivators in vitro. Inactivation assays (200 μl) contained recombinant CYP2C8 (100 pmol/ml) or HLMs (1 mg/ml), NADPH-regenerating system and selected inactivators (at least 5 different concentrations) in phosphate buffer (0.1 M, pH 7.4). At selected pre-incubation times, a 20 μl aliquot was removed and diluted 10-fold to the activity assay containing either 30 μM (recombinant CYP2C8) or 100 μM (HLMs) paclitaxel and NADPH-regenerating system. Reactions were terminated after 10 min and the concentration of the 6α- and 3'-phenyl-hydroxylated metabolites of paclitaxel determined by HPLC.

Effect of Trapping Agents and Torsemide on Inactivation of Paclitaxel Metabolism. The inactivation of paclitaxel metabolism by selected drugs was investigated in the presence of the nucleophile trapping agent glutathione (2 mM), the scavengers of reactive oxygen species superoxide dismutase (1000 U/ml) and

mannitol (1mM), and the alternate CYP2C8 substrate, torsemide (500 μM). These components were included individually with drugs in an inactivation assay (10 min) with either recombinant CYP2C8 (100 pmol/ml) or HLMs (1 mg/ml) prior to the determination of remaining paclitaxel 6α- and 3'-phenyl-hydroxylation activity. Control activities were determined in the absence of inactivating drugs.

Effect of Ultrafiltration on Inactivation of Paclitaxel Metabolism. Ultrafiltration studies were performed to determine if the catalytic function of recombinant CYP2C8 could be restored following pre-incubation with putative MBIs. Inactivation assays (250 pmol/ml recombinant CYP2C8) were chilled on ice following a 10 min pre-incubation, transferred to Ultrafree®-MC filters (30,000 NMWL regenerated cellulose membrane; Millipore, Yonezawa, Japan) and centrifuged at 5000 g for 15 min. Samples were washed with 200 μl phosphate buffer (0.1 M, pH 7.4), centrifuged at 5000 g for 30 min and then re-suspended with 200 μl phosphate buffer (0.1 M, pH 7.4). A 20 μl aliquot was removed to determine the rate of 6α-hydroxypaclitaxel formation. Control measurements were performed in the absence of inactivating drugs.

Spectral Difference Scanning. Difference spectra (500 – 380 nm) between reference and sample cuvettes were recorded using a Cary 300 double beam UV-visible spectrophotometer (Varian Inc., Melbourne, Australia). Incubations (500 μl in 0.1 M phosphate buffer, pH 7.4) containing recombinant CYP2C8 (1000 pmol/ml or 2000 pmol/mol for isoniazid), with or without NADPH-regenerating system, were divided into two 250 μl cuvettes. Drugs were added to the sample cuvette (200 μM nortriptyline, 100 μM verapamil, 200 μM fluoxetine, 10 μM amiodarone, 500 μM

isoniazid or 10 μM phenelzine) and an equivalent volume of solvent was added to the reference cuvette. Both were placed in a shaking water bath at 37°C for between 0 – 30 min before difference spectra were recorded. Potassium ferricyanide (200 μM) was then added to both cuvettes and the difference spectrum re-recorded.

Cytochrome P450 Reduced CO-Difference Spectroscopy. Incubations (500 μl in 0.1 M phosphate buffer, pH 7.4) containing recombinant CYP2C8 (1000 pmol/ml), NADPH-regenerating system and inactivating drugs were performed for 10 min at 37ºC and then terminated with 50 μl of ice-cold phosphate buffer (0.1 M pH 7.4) containing 10% glycerol and 1% Emulgen 913. Following the addition of sodium dithionite, the mixture was divided between two 250 μl cuvettes. CO gas was gently bubbled through the sample cuvette for 1 min. The spectrum of the reduced CO-complex was recorded between 500 and 400 nm. Before termination, a 20 μl aliquot was removed to determine the 6α-hydroxypaclitaxel concentration. Control samples were prepared in the absence of inactivating drugs.

HPLC Assays. *Testosterone 6β-hydroxylation (CYP3A4).* 6β-Hydroxytestosterone was quantified by reversed phase HPLC using an Agilent 1100 series HPLC system (Agilent Technologies, Sydney, Australia) fitted with a Waters (Waters, Milford, MA, USA) Nova-Pak C18 column (1.5 cm X 3.9 mm id, 4 μm particle size). The mobile phase, which consisted of water (A) and acetonitrile (B), was delivered at a flow rate of 1 ml/min according to the gradient; initial conditions, 80% A : 20% B changed to 70% A : 30% B over 7 min, then 30% A : 70% B over 1 min which was held for 10 sec before returning to the initial conditions. Retention times of 4-methylumbelliferone (assay internal standard), 6β-hydroxytestosterone and testosterone, measured using

JPET Fast Forward. Published on August 10, 2004 as DOI: 10.1124/jpet.104.071803
This article has not been copyedited and formatted. The final version may differ from this version.

UV detection at 241 nm, were 2.5, 6.2 and 9.8 min, respectively. Concentrations of 6β-hydroxytestosterone in incubations were determined by comparison of the peak area ratios with those of a standard curve.

Paclitaxel 6α-hydroxylation (CYP2C8) and 3'-phenyl-hydroxylation (CYP3A4). 6α- and 3'-phenyl hydroxypaclitaxel were quantified by reversed phase HPLC as described (Kerdpin et al., 2004). Under these conditions, respective retention times for 3'-phenyl-hydroxypaclitaxel, 6α-hydroxypaclitaxel, diethystilbestrol, and paclitaxel were 8.2, 10.6, 12.1 and 14.4 min. 3'-Phenyl-hydroxypaclitaxel and 6α-hydroxypaclitaxel were quantified by using paclitaxel as the standard (Ong et al., 2000).

Data Analysis. All results represent the mean of duplicate determinations. Kinetic constants for paclitaxel 6α- and 3'-phenyl-hydroxylation and testosterone 6β-hydroxylation were derived (EnzFitter, Biosoft, Cambridge, UK) by fitting either to the Michaelis-Menten equation,

$$v = \frac{V_{\max} \times [S]}{K_m + [S]} \qquad (1)$$

where v is the rate of metabolite formation, V_{max} is the maximum velocity, K_m is the Michaelis constant (substrate concentration at half maximal velocity), and [S] is the substrate concentration,

or the Hill equation, which describes sigmoidal kinetics,

$$v = \frac{V_{\max} \times [S]^n}{S_{50}^n + [S]^n} \qquad (2)$$

where S_{50} is the substrate concentration resulting in half maximal velocity and n is the Hill coefficient.

The pre-incubation effect in the initial screen for MBI was determined by subtracting the percent of control activity remaining following pre-incubation from the percent of control activity remaining following co-incubation at the same inhibitor concentration.

Apparent kinetic constants for the inactivation of paclitaxel metabolism were determined using the observed inactivation rate constant (k_{obs}) at each MBI concentration. Since CYP activity declines in the presence of NADPH-regenerating system alone (see Results), control values at each pre-incubation sampling time represent the maximum possible catalytic function at that time (i.e. 100% activity in the absence of MBIs). The values of k_{obs} at each MBI concentration were determined from the slope when the logarithm of the remaining activity as percentage of control was plotted against the pre-incubation time. Inactivation data were fitted to the following equation using nonlinear least squares regression.

$$k_{obs} = \frac{k_{inact} \times [I]}{K_I + [I]} \qquad (3)$$

where k_{inact}, I, and K_I are the maximum rate of inactivation, concentration of inactivator and the inactivator concentration required for half-maximal inactivation.

JPET Fast Forward. Published on August 10, 2004 as DOI: 10.1124/jpet.104.071803
This article has not been copyedited and formatted. The final version may differ from this version.

RESULTS

Expression of Recombinant CYP2C8 and CYP3A4. Levels of expression of CYP2C8/rOxR (328 nmol P450/L culture and 313 nmol rOxR/L culture) and CYP3A4/rOxR (128 nmol P450/L culture and 117 nmol rOxR/L culture) were comparable to those described previously (Boye et al., 2004).

Kinetics of Testosterone and Paclitaxel Metabolism. Available evidence indicates that the conversion of paclitaxel to 6α-hydroxypaclitaxel and 3'-phenyl-hydroxypaclitaxel by HLMs is catalyzed exclusively by CYP2C8 and CYP3A4, respectively (Cresteil et al., 2002; Foti and Fisher, 2003). The identity of 3'-phenyl-hydroxypaclitaxel formed by incubations with HLMs was confirmed using the CYP3A inhibitor troleandomycin. Pre-incubation with 10 μM troleandomycin totally inhibited paclitaxel 3'-phenyl-hydroxylation without affecting the 6α-hydroxylation pathway, consistent with previous observations (Harris et al., 1994). Furthermore, 3'-phenyl-hydroxypaclitaxel was formed in incubations with recombinant CYP3A4 but not by recombinant CYP2C8. The identity of 6α-hydroxypaclitaxel and 6β-hydroxytestosterone was confirmed by reference to authentic standards. The kinetics of paclitaxel 6α-hydroxylation by both HLMs and recombinant CYP2C8 was described by the Michaelis-Menten equation, while testosterone 6β-hydroxylation and paclitaxel 3'-phenyl-hydroxylation formation by HLMs were sigmoidal and described by the Hill equation (Figure 1). Derived kinetic parameters are given in Table 1.

Screening for Pre-Incubation Effects with CYP3A4 and CYP2C8. MBIs exhibit greater inhibition following a pre-incubation step, and this permits screening of drugs to identify and/or confirm a time-dependent component to CYP2C8 and CYP3A4

JPET Fast Forward. Published on August 10, 2004 as DOI: 10.1124/jpet.104.071803
This article has not been copyedited and formatted. The final version may differ from this version.

inhibition. Table 2 shows the percent inhibition difference observed between co- and pre-incubation conditions for the potential inhibitors investigated here.

With the exception of desmethylnortriptyline, desethylamiodarone and indinavir using either recombinant CYP3A4 or HLMs as the enzyme source, and tamoxifen and selegiline using HLMs as the enzyme source, all drugs inhibited testosterone 6β-hydroxylation to a greater extent following pre-incubation compared to co-incubation (i.e., inhibition difference was positive) (Table 2). The macrolide antibiotics (troleandomycin, erythromycin, clarithromycin, roxithromycin and azithromycin) did not inhibit paclitaxel 6α-hydroxylation at concentrations up to 100 μM. The secondary amine tricyclic antidepressants nortriptyline, desipramine, and norclomipramine exhibited positive inhibition differences with paclitaxel 6α-hydroxylation by recombinant CYP2C8. This same pre-incubation effect was not observed with the corresponding tertiary and primary amine tricyclic antidepressants (amitriptyline and desmethylnortriptyline) and was minor (< 10%) with HLMs. The calcium channel blockers diltiazem, verapamil, nicardipine, felodipine and mibefradil and the selective serotonin reuptake inhibitor fluoxetine also showed positive inhibition differences in experiments with recombinant CYP2C8. However, this effect was either reduced or not observed in parallel experiments conducted with HLMs. Consistency between enzyme sources with respect to the observation of a pre-incubation effect was noted for 17α-ethynylestradiol, amiodarone, desethylamiodarone, isoniazid and phenelzine, although the magnitude was generally greater using recombinant enzyme. There was no difference between the co- and pre-incubation inhibition by selegiline, but tranylcypromine showed a negative inhibition difference (i.e., co-incubation inhibition

JPET Fast Forward. Published on August 10, 2004 as DOI: 10.1124/jpet.104.071803
This article has not been copyedited and formatted. The final version may differ from this version.

> pre-incubation inhibition). A pre-incubation effect on paclitaxel 6α-hydroxylation was observed for tamoxifen using HLMs but not with recombinant CYP2C8.

Inactivation Kinetics of Paclitaxel 6α-Hydroxylation Catalyzed by Recombinant CYP2C8. Based on the initial screening results, representative drugs from different therapeutic classes were selected for inactivation studies. Drugs were selected on the basis of inhibitory potency, the magnitude of pre-incubation effect, the apparent disparity between results obtained using recombinant CYP2C8 and HLMs, and the possible mechanistic basis of MBI. Recombinant CYP2C8 activity declined to approximately 35% of original activity when incubated for 30 min in the presence NADPH-regenerating system alone (between day coefficient of variation < 5%). Figure 2 shows the time- and concentration-dependent inhibition of recombinant CYP2C8 by nortripyline, verapamil, fluoxetine, amiodarone, isoniazid and phenelzine, all of which exhibited pseudo first order inactivation kinetics over the pre-incubation times and concentrations studied. Inactivation was saturable in all cases. Kinetic constants for the inactivation of recombinant CYP2C8 by these drugs are presented in Table 3. The rank order of inactivation efficiency was phenelzine > amiodarone > verapamil > nortriptyline > fluoxetine > isoniazid.

Inactivation of Paclitaxel Metabolism by HLMs. The differential metabolism of paclitaxel by CYP2C8 (6α-hydroxylation) and CYP3A4 (3'-phenyl-hydroxylation) was used to assess the possibility of simultaneous MBI in HLMs. CYP2C8 and CYP3A4 activity declined to approximately 55% and 75% of original activity, respectively, when HLMs were incubated for 30 min in the presence of NADPH-regenerating system alone (between day coefficient of variation < 10%). Figure 3 shows the

observed inactivation profiles for the time- and concentration-dependent inhibition of paclitaxel metabolism by amiodarone, isoniazid, and phenelzine. The corresponding inactivation kinetic constants are given in Table 3. Inactivation of human liver microsomal 6α- and 3'-phenyl-hydroxylation was saturable and exhibited pseudo first order inactivation kinetics over the pre-incubation times and concentrations studied. However, the determination of 3'-phenyl-hydroxylation inactivation kinetics by phenelzine was not possible because time-dependent inhibition was only observed at concentrations greater than 10 μM. In contrast to results with recombinant CYP2C8, inhibition of HLM paclitaxel 6α-hydroxylation by nortriptyline, verapamil and fluoxetine was not time-dependent, although verapamil and fluoxetine did inhibit paclitaxel 3'-phenyl-hydroxylation in a manner consistent with MBI (data not shown). K_{inact} / K_I ratios for phenelzine, amiodarone and isoniazid inactivation of paclitaxel 6α-hydroxylation were lower in comparison to recombinant CYP2C8, suggesting reduced efficiency of inactivation. However, the rank order of inactivation efficiency was the same; phenelzine > amiodarone > isoniazid.

Effect of Glutathione, Reactive Oxygen Scavengers and Torsemide on CYP2C8 Inactivation. The addition of glutathione, superoxide dismutase and mannitol to incubations did not prevent or slow inactivation of recombinant CYP2C8 by nortriptyline, verapamil, fluoxetine, amiodarone and isoniazid (Table 4). However, the rate of phenelzine mediated inactivation was reduced in the presence of glutathione and superoxide dismutase, although not by mannitol. Similarly, with the exception of phenelzine, glutathione, superoxide dismutase and mannitol did not prevent or slow CYP2C8 and CYP3A4 inactivation by drugs that were shown to inactivate paclitaxel 6α- and 3'-phenyl-hydroxylation by HLMs (data not shown). Addition of the alternate

CYP2C8 substrate torsemide (500 μM) to incubations prevented or significantly reduced the inactivation of paclitaxel 6α-hydroxylation in all cases (Table 4).

Effect of Ultrafiltration on Recombinant CYP2C8 Inactivation. Recombinant CYP2C8 activity was not restored by ultrafiltration following pre-incubation with nortriptyline, verapamil, fluoxetine and amiodarone (Table 4). The apparent inactivation caused by phenelzine was partially reversed, while full catalytic function was restored in the case of isoniazid (Table 4) and following pre-incubation with trimethoprim, a known reversible CYP2C8 selective inhibitor (data not shown).

Spectral Difference Scanning with Recombinant CYP2C8. Further studies were conducted to investigate whether the inactivation of recombinant CYP2C8 by nortriptyline, verapamil, fluoxetine, amiodarone, isoniazid and phenelzine occurred via the formation of metabolite-intermediate complexes (MICs). Figure 4 shows the spectral difference scans for these six drugs; for clarity only the scans for 10 min incubations are provided. When incubated with recombinant CYP2C8 in the presence of NADPH-regenerating system, nortriptyline, verapamil and fluoxetine showed time-dependent increases in absorbance maxima in the Soret region (456 - 449 nm) that were sensitive to ferricyanide, consistent with MIC formation by alkylamine drugs. Incubations with isoniazid and NADPH-regenerating system resulted in an increase in absorbance between 510 to 420 nm. These spectral changes were sensitive to ferricyanide and transitionary, reaching a maximum by 10 min but then rapidly decreasing. This is consistent with MIC formation by isoniazid observed using rat liver microsomes (Muakkassah et al., 1981). Amiodarone, which contains an amine function, did not form a MIC with recombinant CYP2C8. Rather, there was a NADPH-

JPET Fast Forward. Published on August 10, 2004 as DOI: 10.1124/jpet.104.071803
This article has not been copyedited and formatted. The final version may differ from this version.

dependent but ferricyanide insensitive increase in absorbance with a maximum that shifted from around 435 nm to 428 nm with increasing incubation time. In contrast, phenelzine bound to CYP2C8 in the absence of NADPH-regenerating system to give a typical type II difference binding spectrum with an absorbance maximum at 428 nm. When phenelzine was incubated with NADPH-regenerating system, the absorbance was ferricyanide insensitive and the maximum increased and shifted from 442 nm to 438 nm as incubation time increased.

Reduced CO-Difference Spectra with Recombinant CYP2C8. Reduced CO-difference spectra were recorded following incubations of recombinant CYP2C8 with nortriptyline, verapamil, fluoxetine, amiodarone, isoniazid and phenelzine. Consistent with MIC formation, the decrease in P450 content corresponded to the reduction in paclitaxel 6α-hydroxylation activity following incubations with nortriptyline, verapamil and fluoxetine (Figure 5). For isoniazid, the decrease in P450 content was significantly greater than the reduction in CYP2C8 activity, presumably due to the transient nature of the hydrazide MIC complex. Amiodarone did not decrease P450 content and the majority of the inactivation caused by phenelzine was explained by destruction of the heme component of CYP2C8.

DISCUSSION

The present in vitro studies provide the first data demonstrating MBI of CYP2C8. The overlapping substrate and inhibitor selectivities between CYP3A4 and CYP2C8 were used initially as the basis to screen potential MBIs of CYP2C8. Since MBIs reduce the availability of functional CYP during pre-incubation, greater inhibition following pre-incubation is expected (Silverman, 1988). Using testosterone 6β-hydroxylation, pre-incubation effects were observed for previously described CYP3A4 MBIs, including the macrolide antibiotics (Ito et al., 2003), several calcium channel blockers (Ma et al., 2000), isoniazid (Wen et al., 2002), amiodarone (Ohyama et al., 2000b), fluoxetine (Mayhew et al., 2000), and 17α-ethynylestradiol (Lin et al., 2002). This was not the case for desethylamiodarone, indinavir or the potent reversible inhibitor, ketoconazole. Small pre-incubation effects (< 10%) were observed for the secondary amine TCAs, nortriptyline, desipramine and norclomipramine but the significance of these remains to be fully explored. Consistent with a previous report, tamoxifen showed a pre-incubation effect with recombinant CYP3A4 which was not apparent in corresponding studies with HLMs (Zhao et al., 2002). Greater inhibition of CYP3A4 following pre-incubation was also observed for several MAOIs. Phenelzine was previously shown to cause loss of the heme content of rat microsomal CYP by free radical formation (Muakkassah and Yang, 1981), while selegiline and tranylcypromine were studied as reversible inhibitors of human CYP without consideration of MBI (Taavitsainen et al., 2000; Taavitsainen et al., 2001).

Many of the confirmed CYP3A4 MBIs also demonstrated pre-incubation effects when corresponding screening studies were performed with CYP2C8 (Table 2). Notable exceptions were the macrolide antibiotics, which did not inhibit CYP2C8 (Harris et al.,

1994) and tranylcypromine. Interestingly, desethylamiodarone showed a pre-incubation effect for CYP2C8 but not with CYP3A4. Although consistency between results with recombinant CYP2C8 and HLMs was not always observed, several drugs, including isoniazid, phenelzine, amiodarone, desethylamiodarone and 17α-ethynylestradiol were identified by these initial studies as potentially significant MBIs of CYP2C8.

A weakness of the MBI screening approach is that it is not possible to differentiation between the pre-incubation effects caused by MBI and the pre-incubation effects that may result from the generation of a potent reversible inhibitory metabolite(s). In the absence of a dilution step and using a probe substrate concentration near K_m, an observation of time-dependent inhibition is an indicator of possible MBI rather then verification. Despite this, the approach was validated by correctly confirming or rejecting a drug as a CYP3A4 MBI based on previous reports as described above.

Nortriptyline, verapamil, fluoxetine, and isoniazid may be classified as MBIs of CYP2C8 using recombinant enzyme based on the following observations: (1) Time- and concentration-dependent inhibition (Figure 2); (2) saturable inactivation; (3) inactivation proceeded via a catalytic step(s) as indicated by the requirement of NADPH; (4) inactivation rate was reduced by the alternate substrate torsemide (Table 4); (5) inactivation rate was not reduced in the presence of glutathione and scavengers of reactive oxygen species, suggesting that the production of reactive intermediates remained within the active site prior to inactivation (Table 4); and (6) loss of activity was quasi-irreversible consistent with MIC formation (Figure 4 and Table 4). Many alkylamine drugs are associated with MIC formation and it was therefore not surprising that the inactivation of CYP2C8 by nortriptyline, verapamil,

and fluoxetine, proceeded via this mechanism (Bensoussan et al., 1995). The unusual spectral changes observed for isoniazid were also consistent with the formation of a MIC, albeit from the metabolism of the hydrazide moiety (Muakkassah et al., 1981). Interestingly, disruption of this MIC was possible by ultrafiltration, a characteristic not observed for nortriptyline, verapamil, and fluoxetine (Table 4). The transient nature of the hydrazide MIC and the reversibility of the decrease in P450, observed by the partial restoration of CYP2C8 activity during activity assays (Figure 5), is distinctly different from the more stable MIC formed from alkylamine drugs.

Amiodarone was also expected to form a stable MIC with CYP2C8, given the significant role of CYP2C8 in amiodarone deethylation (Ohyama et al., 2000a), and given that MIC formation by amiodarone in rodents was consistent with tertiary amine metabolism to nitrosoalkane reactive intermediates (Larrey et al., 1986). However, the spectral studies did not detect MIC formation or heme loss (Figure 4 and 5) despite irreversible loss of catalytic function (Table 4). Along with the tertiary amine function, the furan ring in amiodarone is a structural moiety that has previously been associated with MBI. However, metabolism of the furan ring of furafylline was recently excluded as a basis for CYP1A2 inactivation (Racha et al., 1998). Furthermore, other furan containing drugs, such as methoxsalen, are potent suicide inhibitors associated with loss of spectrally observable heme (Tinel et al., 1987), a feature not observed here. Thus, the exact mechanism by which amiodarone inactivates CYP2C8 remains unclear, although covalent binding to the CYP2C8 apoprotein may explain the NADPH-dependent spectral differences observed.

Although fulfilling several in vitro MBI criteria, the inactivation of recombinant and human liver microsomal CYP2C8 by phenelzine was not, strictly speaking,

JPET Fast Forward. Published on August 10, 2004 as DOI: 10.1124/jpet.104.071803
This article has not been copyedited and formatted. The final version may differ from this version.

mechanism-based. Inactivation rate was reduced in the presence of the nucleophile glutathione and the reactive oxygen species scavenger superoxide dismutase, indicating that reactive intermediates escape the active site prior to inactivation (Table 4). Consistent with these observations, heme destruction via free radical formation during oxidation of phenelzine has been proposed previously (Muakkassah and Yang, 1981). In addition, a potent reversible metabolite(s) appears to contribute towards time-dependent inhibition because activity was partially restored by ultrafiltration (Table 4). Such free radicals and metabolite(s) are likely to cause inhibition and inactivation of other CYP enzymes. Hence, phenelzine should be considered a metabolically activated inactivator (Silverman, 1988).

The differential metabolism of paclitaxel by HLMs was used to study the kinetics of simultaneous CYP2C8 and CYP3A4 inactivation by amiodarone, isoniazid and phenelzine (Figure 3). Although Foti and Fisher (2003) recently reported the 3'-phenyl-hydroxylation pathway as a metabolic route specific to CYP3A4 and not CYP3A5, the 3'-phenyl-hydroxylation inactivation kinetic constants obtained here for verapamil, fluoxetine and amiodarone agree well with those reported using the non-selective CYP3A substrates midazolam and testosterone (Mayhew et al., 2000; Ohyama et al., 2000b; Wang et al., 2004). The efficiency of CYP3A4 inactivation was greater compared to CYP2C8 for all three drugs tested, although inter-enzyme comparisons were not possible for phenelzine. The k_{inact} / K_I ratio is used to evaluate the potential clinical impact of MBI (Lu et al., 2003). In comparison to other clinically significant MBIs, k_{inact} / K_I ratios for the effects of amiodarone and isoniazid on human liver microsomal paclitaxel 6α-hydroxylation are low. It is therefore unlikely that these drugs would significantly reduce the in vivo clearance of other CYP2C8 substrates. However, inactivation of CYP2C8 by phenelzine was comparable to CYP3A4

JPET Fast Forward. Published on August 10, 2004 as DOI: 10.1124/jpet.104.071803
This article has not been copyedited and formatted. The final version may differ from this version.

inactivation by erythromycin, a drug commonly associated with CYP3A4-mediated drug-drug interactions (Ito et al., 2003).

In contrast to results with recombinant CYP2C8, nortriptyline, verapamil and fluoxetine were not MBIs of the human liver microsomal isoform. Furthermore, the efficiency of inactivation was reduced for amiodarone, isoniazid and phenelzine, as reflected by lower k_{inact} / K_I ratios. Similar discrepancies between recombinant and human liver microsomal MBI kinetic data have been noted previously for 5-fluoro-2-[4-[(2-phenyl-1H-imidazol-5-yl)methyl]-1-piperazinyl]pyrimidine, (SCH 66712), tamoxifen and verapamil (Palamanda et al., 2001; Zhao et al., 2002; Wang et al., 2004). This may arise from the non-specific binding of certain drugs to HLMs, which would effectively lower the 'available' concentration present in incubations and confound the determination of kinetic constants. In comparing the results for HLMs and recombinant CYP2C8, the higher apparent K_m for paclitaxel 6α-hydroxylation, the smaller pre-incubation effects observed during the MBI screen, and the greater K_I values for amiodarone and phenelzine all provide supporting evidence for this hypothesis. Despite this, the exact differences (if any) between the binding of drugs to human liver microsomes and *E. coli* membrane fractions are unknown. Alternatively, Palamanda et al. (2001) suggest that sufficient catalytic turnover to the reactive intermediate occurs with the isolated recombinant enzyme, whereas these reactions are of lesser significance due to competing metabolic pathways in HLMs that lower the MBI concentration. However, both these explanations fail to explain the results for nortriptyline, verapamil and fluoxetine. Time-dependent inhibition of CYP2C8 in HLMs was not observed despite a significant component of reversible inhibition at concentrations that resulted in MBI of recombinant CYP2C8 (data not shown). Hence, concentration was not limiting in the presence of other enzymes or

considering the likely non-specific binding of these drugs in HLMs. Thus, the exact reason(s) why some drugs behave as in vitro MBIs using recombinant systems without the corresponding effect on the human liver microsomal enzyme remains an intriguing question.

In conclusion, we have demonstrated that CYP2C8 is susceptible to MBI by drugs that are common CYP3A4 inhibitors, several of which have been implicated in clinically important drug-drug interactions. Data are consistent with MBI of recombinant CYP2C8 by nortriptyline, verapamil, fluoxetine, amiodarone and isoniazid, while phenelzine acts as a metabolically activated inactivator. Studies with HLMs revealed that nortriptyline, verapamil and fluoxetine were not MBIs of CYP2C8, while simultaneous inactivation of CYP2C8 and CYP3A4 was described using amiodarone, isoniazid and phenelzine. Inactivation of human CYP by commonly prescribed drugs may be more widespread then currently believed.

REFERENCES

Bensoussan C, Delaforge M and Mansuy D (1995) Particular ability of cytochromes P450 3A to form inhibitory P450-iron-metabolite complexes upon metabolic oxidation of aminodrugs. *Biochem Pharmacol* **49**:591-602.

Bertelsen KM, Venkatrishnan K, von Moltke LL, Obach RS and Greenblatt DJ (2003) Apparent mechanism-based inhibition of human CYP2D6 in vitro by paroxetine: comparison with fluoxetine and quinidine. *Drug Metab Dispos* **31**:289-293.

Bidstrup TB, Bjornsdottir I, Sidelmann UG, Thomsen MS and Hansen KT (2003) CYP2C8 and CYP3A4 are the principal enzymes involved in the human in vitro biotransformation of the insulin secretagogue repaglinide. *Br J Clin Pharmacol* **56**:305-314.

Boye SL, Kerdpin O, Elliot DJ, Miners JO, Kelly L, McKinnon RA, Bhasker CR, Yoovathaworn K and Birkett DJ (2004) Optimizing bacterial expression of catalytically active human cytochromes P450: comparison of CYP2C8 and CYP2C9. *Xenobiotica* **34**:49-60.

Cresteil T, Monsarrat B, Dubois J, Sonnier M, Alvinerie P and Gueritte F (2002) Regioselective metabolism of taxoids by human CYP3A4 and 2C8: structure-activity relationship. *Drug Metab Dispos* **30**:438-445.

Desta Z, Wu GM, Morocho AM and Flockhart DA (2002) The gastroprokinetic and antiemetic drug metoclopramide is a substrate and inhibitor of cytochrome P450 2D6. *Drug Metab Dispos* **30**:336-343.

Foti RS and Fisher MB (2003) Characterisation of cytochrome P450 3A4 and 3A5 levels in a human liver microsome bank using midazolam and paclitaxel metabolic acitivity and immunoquantitation. *Drug Metab Rev* **35**:34.

Ha-Duong NT, Dijols S, Macherey AC, Goldstein JA, Dansette PM and Mansuy D (2001) Ticlopidine as a selective mechanism-based inhibitor of human cytochrome P450 2C19. *Biochemistry* **40**:12112-12122.

Harris JW, Rahman A, Kim BR, Guengerich FP and Collins JM (1994) Metabolism of taxol by human hepatic microsomes and liver slices: participation of cytochrome P450 3A4 and an unknown P450 enzyme. *Cancer Res* **54**:4026-4035.

Ito K, Ogihara K, Kanamitsu S and Itoh T (2003) Prediction of the in vivo interaction between midazolam and macrolides based on in vitro studies using human liver microsomes. *Drug Metab Dispos* **31**:945-954.

Kerdpin O, Elliot DJ, Boye SL, Birkett DJ, Yoovathaworn K and Miners JO (2004) Differential contribution of active site residues in substrate recognition sites 1 and 5 to cytochrome P450 2C8 substrate- and regio-selectivity. *Biochemistry* **43**:7834-7842.

Koudriakova T, Iatsimirskaia E, Utkin I, Gangl E, Vouros P, Storozhuk E, Orza D, Marinina J and Gerber N (1998) Metabolism of the human immunodeficiency virus protease inhibitors indinavir and ritonavir by human intestinal microsomes and expressed cytochrome P4503A4/3A5: mechanism-based inactivation of cytochrome P4503A by ritonavir. *Drug Metab Dispos* **26**:552-561.

Larrey D, Tinel M, Letteron P, Geneve J, Descatoire V and Pessayre D (1986) Formation of an inactive cytochrome P-450Fe(II)-metabolite complex after administration of amiodarone in rats, mice and hamsters. *Biochem Pharmacol* **35**:2213-2220.

Lin HL, Kent UM and Hollenberg PF (2002) Mechanism-based inactivation of cytochrome P450 3A4 by 17 alpha-ethynylestradiol: evidence for heme destruction and covalent binding to protein. *J Pharmacol Exp Ther* **301**:160-167.

Lin JH and Lu AY (1998) Inhibition and induction of cytochrome P450 and the clinical implications. *Clin Pharmacokinet* **35**:361-390.

Lowry OH, Rosenbrough NJ, Farr L and Randall RJ (1951) Protein Measurement with the Folin Phenol Reagent. *J Biol Chem* **193**:267-275.

Lu P, Schrag ML, Slaughter DE, Raab CE, Shou M and Rodrigues AD (2003) Mechanism-based inhibition of human liver microsomal cytochrome P4501A2 by zileuton, a 5-lipoxygenase inhibitor. *Drug Metab Dispos* **31**:1352-1360.

Ma B, Prueksaritanont T and Lin JH (2000) Drug interactions with calcium channel blockers: possible involvement of metabolite-intermediate complexation with CYP3A. *Drug Metab Dispos* **28**:125-130.

Mayhew BS, Jones DR and Hall SD (2000) An in vitro model for predicting in vivo inhibition of cytochrome P450 3A4 by metabolic intermediate complex formation. *Drug Metab Dispos* **28**:1031-1037.

Muakkassah SF, Bidlack WR and Yang WC (1981) Mechanism of the inhibitory action of isoniazid on microsomal drug metabolism. *Biochem Pharmacol* **30**:1651-1658.

Muakkassah SF and Yang WC (1981) Mechanism of the inhibitory action of phenelzine on microsomal drug metabolism. *J Pharmacol Exp Ther* **219**:147-155.

O'Donnell JP, Dalvie DK, Kalgutkar AS and Obach RS (2003) Mechanism-based inactivation of human recombinant P450 2C9 by the nonsteroidal anti0inflammatory drug suprofen. *Drug Metab Dispos* **31**:1369-1377.

Ohyama K, Nakajima M, Nakamura S, Shimada N, Yamazaki H and Yokoi T (2000a) A significant role of human cytochrome P450 2C8 in amiodarone N-deethylation: an approach to predict the contribution with relative activity factor. *Drug Metab Dispos* **28**:1303-1310.

Ohyama K, Nakajima M, Suzuki M, Shimada N, Yamazaki H and Yokoi T (2000b) Inhibitory effects of amiodarone and its N-deethylated metabolite on human cytochrome P450 activities: prediction of in vivo drug interactions. *Br J Clin Pharmacol* **49**:244-253.

Omura T and Sato R (1964) The Carbon Monoxide-binding Pigment of Liver Microsomes. *J Biol Chem* **239**:2379-2385.

Ong CE, Coulter S, Birkett DJ, Bhasker CR and Miners JO (2000) The xenobiotic inhibitor profile of cytochrome P4502C8. *Br J Clin Pharmacol* **50**:573-580.

Palamanda JR, Casciano CN, Norton LA, Clement RP, Favreau LV, Lin C and Nomeir AA (2001) Mechanism-based inactivation of CYP2D6 by 5-fluoro-2-[4-[(2-phenyl-1H-imidazol-5-yl)methyl]-1-piperazinyl]pyrimidine. *Drug Metab Dispos* **29**:863-867.

Projean D, Baune B, Farinotti R, Flinois JP, Beaune P, Taburet AM and Ducharme J (2003) In vitro metabolism of chloroquine: identification of CYP2C8, CYP3A4, and CYP2D6 as the main isoforms catalyzing N-desethylchloroquine formation. *Drug Metab Dispos* **31**:748-754.

Racha JK, Rettie AE and Kunze KL (1998) Mechanism-based inactivation of human cytochrome P450 1A2 by furafylline: detection of a 1:1 adduct to protein and evidence for the formation of a novel imidazomethide intermediate. *Biochemistry* **37**:7407-7419.

Richardson TH, Jung F, Griffin KJ, Wester M, Raucy JL, Kemper B, Bornheim LM, Hassett C, Omiecinski CJ and Johnson EF (1995) Universal Approach to the Expression of Human and Rabbit Cytochrome P450s of the 2c Subfamily in Escherichia Coli. *Arch Biochem Biophys* **323**:87-96.

Richter T, Murdter TE, Heinkele G, Pleiss J, Tatzel S, Schwab M, Eichelbaum M and Zanger UM (2004) Potent mechanism-based inhibition of human CYP2B6 by clopidogrel and ticlopidine. *J Pharmacol Exp Ther* **308**:189-197.

Silverman RB (1988) *Mechanism-Based Enzyme Inactivation: Chemistry and Enzymology*. CRC Press, Inc. Boca Raton, Florida.

Taavitsainen P, Anttila M, Nyman L, Karnani H, Salonen JS and Pelkonen O (2000) Selegiline metabolism and cytochrome P450 enzymes: in vitro study in human liver microsomes. *Pharmacol Toxicol* **86**:215-221.

Taavitsainen P, Juvonen R and Pelkonen O (2001) In vitro inhibition of cytochrome P450 enzymes in human liver microsomes by a potent CYP2A6 inhibitor, trans-2-phenylcyclopropylamine (tranylcypromine), and its nonamine analog, cyclopropylbenzene. *Drug Metab Dispos* **29**:217-222.

Tinel M, Belghiti J, Descatoire V, Amouyal G, Letteron P, Geneve J, Larrey D and Pessayre D (1987) Inactivation of human liver cytochrome P-450 by the drug methoxsalen and other psoralen derivatives. *Biochem Pharmacol* **36**:951-955.

Wang JS and DeVane CL (2003) Involvement of CYP3A4, CYP2C8, and CYP2D6 in the metabolism of (R)- and (S)-methadone in vitro. *Drug Metab Dispos* **31**:742-747.

Wang Y, Jones DR and Hall SD (2004) Prediction of cytochrome P450 3A inhibition by verapamil enantiomers and their metabolites. *Drug Metab Dispos* **32**:259-266.

Wen X, Wang JS, Neuvonen PJ and Backman JT (2002) Isoniazid is a mechanism-based inhibitor of cytochrome P450 1A2, 2A6, 2C19 and 3A4 isoforms in human liver microsomes. *Eur J Clin Pharmacol* **57**:799-804.

Yasukochi Y and Masters BS (1976) Some properties of a detergent-solubilized NADPH-cytochrome c(cytochrome P-450) reductase purified by biospecific affinity chromatography. *J Biol Chem* **251**:5337-5344.

Zhao XJ, Jones DR, Wang YH, Grimm SW and Hall SD (2002) Reversible and irreversible inhibition of CYP3A enzymes by tamoxifen and metabolites. *Xenobiotica* **32**:863-878.

FOOTNOTES

This work was supported by a grant from the National Health and Medical Research Council of Australia. T.M.P. is the recipient of an Australian Post-Graduate Award.

a) Part of this work will be presented at the 8th World Congress of Clinical Pharmacology and Therapeutics, Brisbane, Australia, August 1st - 6th, 2004, and at the 7th International ISSX Meeting, Vancouver, Canada, August 29th - September 3rd, 2004.

b) Reprint Requests: Professor John O. Miners, Department of Clinical Pharmacology, Flinders University and Flinders Medical Centre, Bedford Park, SA 5042, Australia. Telephone: 61-8-82044999. Fax: 61-8-82045114. Email: John.Miners@flinders.edu.au

LEGENDS FOR FIGURES

Figure 1: Representative Eadie-Hofstee plots for paclitaxel 6α-hydroyxlation by (a) recombinant CYP2C8 and (b) HLMs (H40), and paclitaxel 3'-phenyl-hydroxylation by (c) HLMs (H40). Points are experimentally determined values (means of duplicate measurements at each concentration) while the solid lines are the computer-generated curves of best fit.

Figure 2: Time- and concentration-dependent inactivation of recombinant CYP2C8 catalyzed paclitaxel 6α-hydroylation after incubations with nortriptyline, verapamil, fluoxetine, amiodarone, isoniazid and phenelzine. Aliquots (20 μl) were removed from the primary reaction mixture at the indicated time points and assayed for residual CYP2C8 activity. Derived kinetic constants for the inactivation of CYP2C8 were determined as described in *Materials and Methods*.

Figure 3: Simultaneous inactivation of CYP2C8-mediated paclitaxel 6α-hydroylation (solid triangles) and CYP3A4-mediated paclitaxel 3'-phenyl-hydroylation (solid squares) by amiodarone, isoniazid and phenelzine in HLMs. Aliquots (20 μl) were removed from the primary reaction mixture at selected time points and assayed for residual paclitaxel 6α-hydroxylation and 3'-phenyl-hydroxylation activity. Observed inactivation rates at each inactivator concentration were obtained from the slope when the logarithm of the remaining activity as percentage of control was plotted against the pre-incubation time. Derived kinetic constants for the inactivation of CYP2C8 and CYP3A4 were determined as described in *Materials and Methods*. Points are experimentally determined values (means of duplicate measurements at

each concentration) while the solid lines are the computer-generated curves of best fit.

Figure 4: Representative 10 min difference spectra for incubations of recombinant CYP2C8 with nortriptyline, verapamil, fluoxetine, amiodarone, isoniazid and phenelzine in the absence (thin sold line) or presence of NADPH-regenerating system (thick solid line) and following the addition of potassium ferricyanide (dashed line).

Figure 5: Recombinant CYP2C8 P450 content and rate of paclitaxel 6α-hydroxylation following incubations with nortriptyline, verapamil, fluoxetine, amiodarone, phenelzine and isoniazid.

JPET Fast Forward. Published on August 10, 2004 as DOI: 10.1124/jpet.104.071803
This article has not been copyedited and formatted. The final version may differ from this version.

TABLE 1

Derived kinetic constants for paclitaxel and testosterone hydroxylation by recombinant enzymes and human liver microsomes

Substrate velocity data was fitted either to the Michaelis-Menten or Hill equations and kinetic constants determined as described in *Materials and Methods*. Data represent the mean (± SD) of five separate determinations with recombinant enzymes and six (testosterone 6β-hydroxylation and paclitaxel 6α-hydroxylation) or three (paclitaxel 3'-phenyl-hydroxylation) separate determinations for microsomes from human livers.

	CYP2C8	CYP3A4	Human Liver Microsomes		
	Paclitaxel 6α-hydroxylation	Testosterone 6β-hydroxylation	Testosterone 6β-hydroxylation	Paclitaxel 6α-hydroxylation	Paclitaxel 3'-phenyl-hydroxylation
K_m (μM)	1.51 ± 0.25			7.50 ± 1.08	
S_{50} (μM)		32.3 ± 2.8	35.6 ± 4.3		13.2 ± 3.3
V_{max} [a]	2.94 ± 0.50	35.2 ± 2.3	2413 ± 90	70.2 ± 29.3	29.1 ± 7.9
n [b]		1.33 ± 0.06	1.39 ± 0.05		1.29 ± 0.06

[a] V_{max} = pmol/min/pmol recombinant CYP or pmol/min/mg human liver microsomal protein.

[b] Hill Coefficient

JPET Fast Forward. Published on August 10, 2004 as DOI: 10.1124/jpet.104.071803
This article has not been copyedited and formatted. The final version may differ from this version.

TABLE 2

Screening for potential MBI of CYP3A4 and CYP2C8

Drugs were co- and pre-incubated as described in *Materials and Methods* and the inhibition difference between co- and pre-incubation conditions determined. Data represent the mean of at least duplicate determinations.

	Testosterone 6β-Hydroxylation			Paclitaxel 6α-Hydroxylation		
	Conc. (μM)	Inhibition Difference (as % of Control)		Conc. (μM)	Inhibition Difference (as % of Control)	
Drug		Recombinant CYP3A4	HLMs		Recombinant CYP2C8	HLMs
Macrolides						
Troleandomycin	1	25.6	39.9	10	*N/O*	*N/O*
	10	17.8	24.4	100	*N/O*	*N/O*
Erythromycin	20	33.0	25.8	10	*N/O*	*N/O*
	100	11.7	21.3	100	*N/O*	*N/O*
Clarithromycin	20	32.7	24.0	10	*N/O*	*N/O*
	100	14.8	28.4	100	*N/O*	*N/O*
Roxithromycin	20	21.4	10.2	10	*N/O*	*N/O*
	100	11.9	9.3	100	*N/O*	*N/O*
Azithromycin	20	24.3	5.7	10	*N/O*	*N/O*
	100	14.3	18.3	100	*N/O*	*N/O*
TCAs						
Amitriptyline	5	2.1	-0.1	50	2.3	-5.1
	20	0.3	1.5	400	0.2	-0.9
Nortriptyline	5	9.4	4.1	50	22.7	3.6
	20	9.0	3.6	400	13.2	5.0
Desmethylnortriptyline	5	-8.4	-1.9	5	-22.0	-11.2
	20	-10.2	-5.7	20	-18.1	-0.8
Desipramine	5	11.6	5.6	50	13.1	8.5
	20	0.9	3.9	400	20.0	9.0
Norclomipramine	5	8.8	1.5	50	39.2	8.3

JPET Fast Forward. Published on August 10, 2004 as DOI: 10.1124/jpet.104.071803
This article has not been copyedited and formatted. The final version may differ from this version.

	20	8.4	1.5	400	46.6	-0.1
CCBs						
Diltiazem	1	12.4	6.9	100	34.6	*N/D*
	5	12.3	16.3	250	19.7	*N/D*
Verapamil	1	22.2	18.4	20	74.3	1.1
	5	44.7	33.0	100	42.4	0
Nicardipine	0.5	22.9	34.6	1	14.1	-2.6
	2	12.6	10.7	5	8.0	-0.9
Felodipine	2	12.6	14.5	0.5	0	3.6
	10	4.1	13.6	2	20.7	9.3
Mibefradil	0.1	25.5	46.8	2	34.0	2.3
	0.5	11.9	29.9	10	29.6	0
MAOIs						
Selegiline	20	6.5	0.5	20	1.0	-3.2
	100	19.9	0	100	0.2	1.0
Tranylcypromine	20	10.1	-6.7	20	-24.0	-24.3
	100	7.5	3.3	100	-9.4	-7.9
Phenelzine	5	10.8	23.9	5	43.5	11.9
	20	10.8	12.5	20	29.4	42.8
Miscellaneous CYP3A4 Inhibitors						
Isoniazid	20	24.9	15.9	20	19.4	2.9
	100	8.1	7.1	100	15.6	6.5
17α-Ethynylestradiol	10	7.0	26.8	1	22.9	12.7
	50	14.7	12.2	5	19.0	7.7
Amiodarone	10	15.6	5.7	1	51.0	18.0
	50	18.0	9.8	5	26.9	36.0
Desethylamiodarone	1	-1.1	-5.0	0.5	41.9	14.1
	5	-1.0	-1.7	2	35.6	14.1
Indinavir	0.1	-28.0	-2.6	10	-5.0	-5.5

	1	-18.0	-6.1	100	-16.7	-4.3
Fluoxetine	1	7.5	8.7	100	69.2	1.8
	5	12.6	13.1	250	60.7	1.2
Tamoxifen	5	10.2	-7.0	5	-5.8	10.3
	25	7.2	-3.2	25	-6.4	13.0
Negative Controls						
Ketoconazole	0.005	*N/D*	-4.8			
Torsemide				150	-6.4	*N/D*

N/O = co- and pre-incubation inhibition not observed.
N/D = not determined.

JPET Fast Forward. Published on August 10, 2004 as DOI: 10.1124/jpet.104.071803
This article has not been copyedited and formatted. The final version may differ from this version.

TABLE 3

Derived kinetic constants for the inactivation of paclitaxel metabolism by selected drugs

K_I and k_{inact} were determined as described in *Materials and Methods*.

	Recombinant CYP2C8			Human Liver Microsomes					
	Paclitaxel 6α-hydroxylation			Paclitaxel 6α-hydroxylation			Paclitaxel 3'-phenyl-hydroxylation		
	K_I (μM)	k_{inact} (min^{-1})	k_{inact}/K_I ($min^{-1}\,\mu M^{-1}$)	K_I (μM)	k_{inact} (min^{-1})	k_{inact}/K_I ($min^{-1}\,\mu M^{-1}$)	K_I (μM)	k_{inact} (min^{-1})	k_{inact}/K_I ($min^{-1}\,\mu M^{-1}$)
Nortriptyline	49.9	0.036	0.00072	*N/O*	*N/O*	*N/O*	*N/O*	*N/O*	*N/O*
Verapamil	17.5	0.065	0.00371	*N/O*	*N/O*	*N/O*	4.2	0.092	0.02190
Fluoxetine	294	0.083	0.00028	*N/O*	*N/O*	*N/O*	21.2	0.018	0.00085
Amiodarone	1.5	0.079	0.05374	51.2	0.029	0.00057	10.2	0.032	0.00314
Isoniazid	374	0.042	0.00011	170	0.012	0.00007	28.4	0.065	0.00229
Phenelzine	1.2	0.243	0.19918	54.3	0.17	0.00313	*N/D*	*N/D*	*N/D*

N/O = time dependent inhibition not observed.
N/D = not determined.

JPET Fast Forward. Published on August 10, 2004 as DOI: 10.1124/jpet.104.071803
This article has not been copyedited and formatted. The final version may differ from this version.

TABLE 4

Effect of glutathione, scavengers of reactive oxygen species, torsemide and ultrafiltration on the inactivation of recombinant CYP2C8 by selected drugs

CYP2C8 was pre-incubated with inhibitor for 10 min at 37°C. Control preparations were pre-incubated with NADPH-regenerating system alone and either glutathione, superoxide dismutase, mannitol or torsemide but lacking test drug. Directly following pre-incubation or following ultrafiltration and re-suspension, aliquots were removed and diluted 10-fold to determine paclitaxel 6α-hydroxylation rate. Data represent the mean of duplicate determinations.

	Paclitaxel 6α-hydroxylation Rate (% of Control)					
	NADPH	NADPH + Glutathione (2 mM)	NADPH + Superoxide Dismutase (1000 U/ml)	NADPH + Mannitol (1mM)	NADPH + Torsemide (500 μM)	NADPH + Ultrafiltration
Control	100	100	100	100	100	100
Nortriptyline (200 μM)	67.1	67.4	65.4	61.4	106.7	56.6
Verapamil (100 μM)	44.4	42.7	49.2	45.5	98.5	34.7
Fluoxetine (200 μM)	46.4	53.9	46.4	48.5	101.7	41.3
Amiodarone (4 μM)	38.8	33.1	37.4	38.7	108.4	29.0
Isoniazid (500 μM)	70.4	67.8	68.5	67.7	91.3	108.4
Phenelzine (4 μM)	14.1	77.1	93.3	13.2	94.3	53.6

JPET Fast Forward. Published on August 10, 2004 as DOI: 10.1124/jpet.104.071803
This article has not been copyedited and formatted. The final version may differ from this version.

JPET #71803

Figure 1

(a)

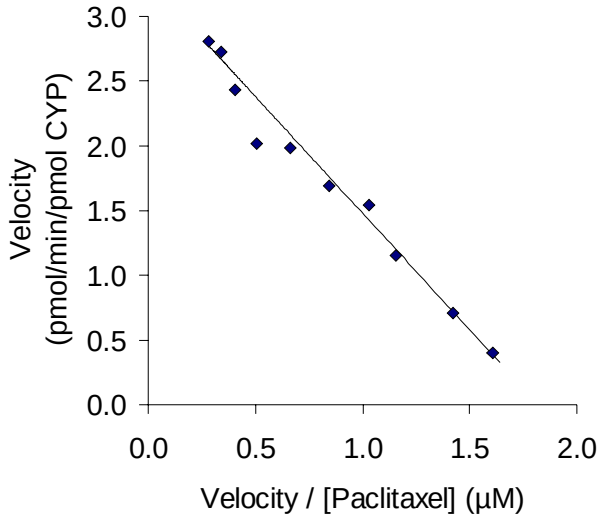

(b)

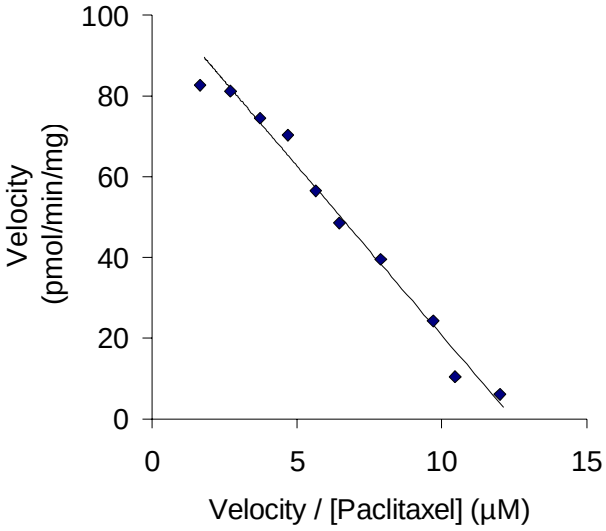

(c)

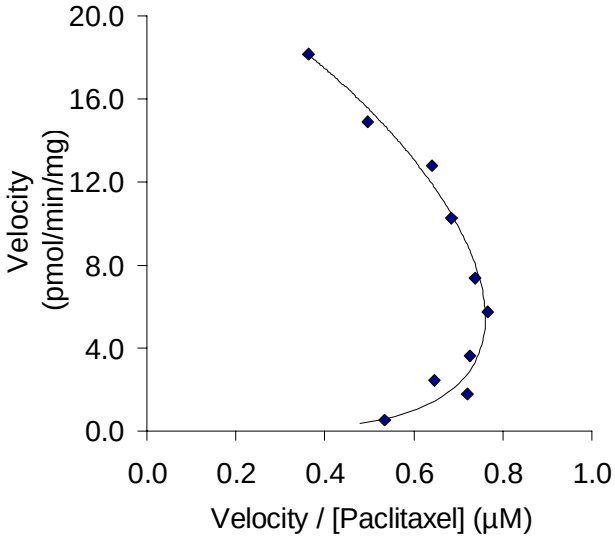

JPET Fast Forward. Published on August 10, 2004 as DOI: 10.1124/jpet.104.071803
This article has not been copyedited and formatted. The final version may differ from this version.

JPET #71803

Figure 2

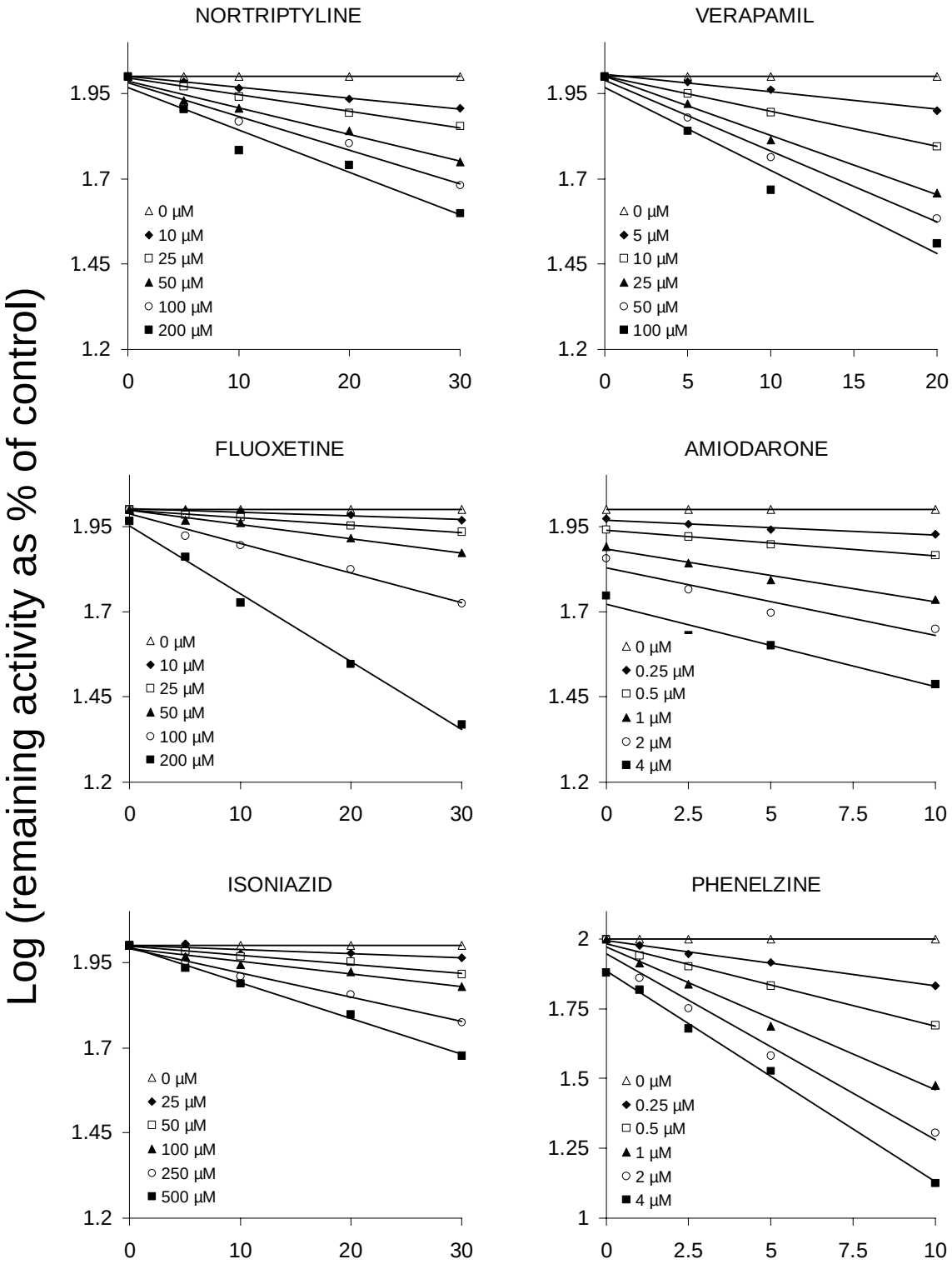

JPET Fast Forward. Published on August 10, 2004 as DOI: 10.1124/jpet.104.071803
This article has not been copyedited and formatted. The final version may differ from this version.

JPET #71803

Figure 3

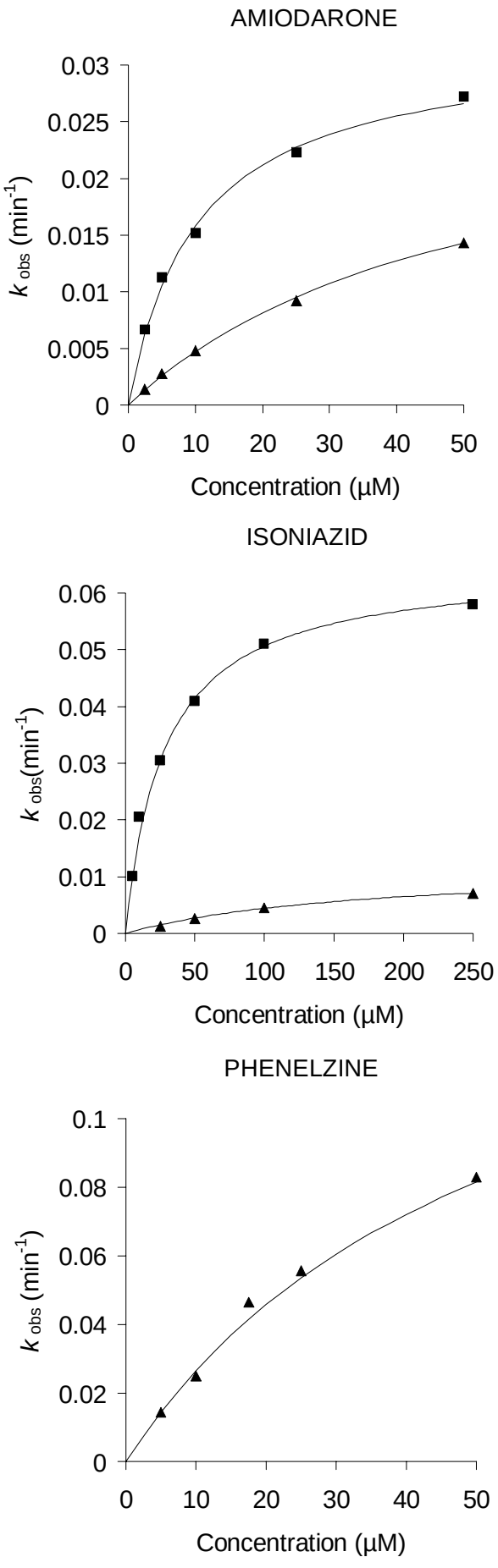

JPET Fast Forward. Published on August 10, 2004 as DOI: 10.1124/jpet.104.071803
This article has not been copyedited and formatted. The final version may differ from this version.

JPET #71803

Figure 4

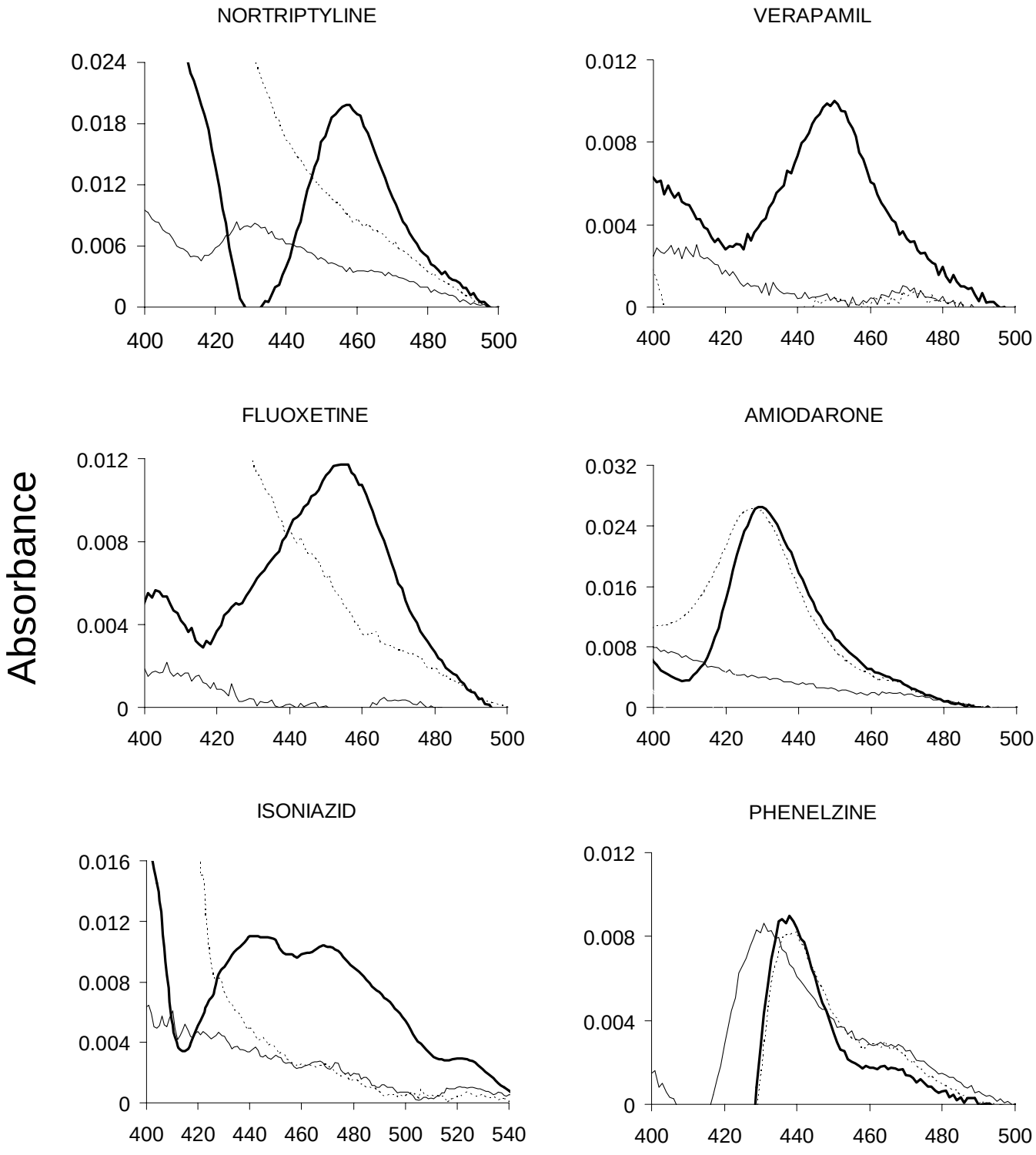

JPET Fast Forward. Published on August 10, 2004 as DOI: 10.1124/jpet.104.071803
This article has not been copyedited and formatted. The final version may differ from this version.

JPET #71803

Figure 5